



Cathodic Cleaning of Oxides from Aluminum Surface by Variable-Polarity Arc

Direct real-time observation by a high-speed machine vision system shows the role of cathode spots in the cathodic cleaning of oxides and their behavior during the cleaning process

BY R. SARRAFI AND R. KOVACEVIC

ABSTRACT

In-process cleaning of oxides facilitates the high-quality welding and cladding of aluminum alloys when GTAW arc is used for melting aluminum in an open atmosphere. However, in order to understand the mechanism of cathodic cleaning, direct observation is needed. In this work, in order to visualize the physical processes underlying cathodic cleaning, a machine-vision system is developed, and the interaction of the variable-polarity arc with the aluminum surface is captured in real time by a high-speed camera. Surface studies are also performed to assist with the understanding of the oxide cleaning process. Real-time images and surface topography suggest that the cathode spots are responsible for removing oxides from the cathode surface during direct current electrode positive (DCEP) polarity. The cathodically cleaned zone expands over time. However, after the diameter of the cleaned zone reaches a specific value, the rate of its expansion decreases and stops. Unlike cathode spots of vacuum arc, the cathode spots of atmospheric welding arc form on the surface with original oxides, as well as on the surface already scanned by cathode spots (possibly because of the re-formation of a thin layer of oxides on the surface). Two phases of cathode spot behavior were observed during each pulse of DCEP polarity. In the first phase, small spots scan the surface

with a very high speed. In the second phase, larger spots form on the area previously scanned during the first phase and move outward with a slower speed. Among the process parameters, the duration of the DCEP polarity (the DCEP duty cycle) has the most significant effect on the size of the cleaned zone and its rate of growth.

Introduction

In-process removal of surface oxides is a very important element of the welding procedure when high-quality welds or deposits of aluminum alloys are to be achieved by gas tungsten arc welding (GTAW) in an open atmosphere. The melting temperature of aluminum oxide (2050°C) is much higher than that of aluminum alloys. The high melting temperature of aluminum oxide and its tenacious behavior in the weld pool can cause weld defects. The presence of the oxide layer on the molten pool can cause fusion defects (Refs. 1, 2), inclusions, and porosities (Refs. 1, 3).

To remove the oxides during melting of aluminum alloys by GTAW, alternative current can be used. During the direct current electrode positive (DCEP) polarity of the arc, the cathodic cleaning of oxides occurs. Because of the oxide cleaning function of the variable-polarity arc during DCEP polarity, variable-polarity plasma arc welding (VP PAW) and variable-po-

larity gas tungsten arc welding (VP GTAW) are used for high-quality welding, cladding (Refs. 4, 5), and rapid prototyping (Refs. 6, 7) of aluminum alloys.

There are some reports in the literature discussing the feasibility of methods for real-time oxide cleaning during aluminum melting other than cathodic cleaning. Jarvis and Ahmed (Ref. 8) showed that the oxides can be thermally removed by a direct current electrode negative (DCEN) arc under helium shielding gas. Ryazantsev et al. (Ref. 9) showed that the oxides can be partially removed by the forces induced by the fluid flow in the molten pool. However, the success and popularity of these methods are far less than oxide cleaning by using the DCEP polarity of the arc.

Background information on the physics of atmospheric arcs is needed to study the mechanism of cathodic cleaning. Therefore, before discussing the possible mechanisms of cathodic cleaning, some basic information on arc physics is presented in the next few sections.

Arc Cathode Physics

The typical distribution of voltage across the arc plasma is shown in Fig. 1. There is a sharp gradient of voltage in the vicinity of both electrodes (cathode and anode). The potential gradient in the vicinity of the cathode is called cathode fall voltage, which is in the range of 10 to 20 V for the welding arc (Ref. 10), and is greater than the voltage gradient near the anode. The cathode fall zone acts as a transition zone between the metallic and plasma states and is necessary for sustaining the arc on the cathode.

As schematically shown in Fig. 2, the cathode fall zone has an internal structure and consists of two distinct zones (Ref. 11): the cathode sheath (or cathode space charge zone), and presheath (or ionization

KEYWORDS

Cathodic Cleaning
Oxides
Arc Physics
Variable Polarity
Aluminum Welding

R. SARRAFI (rsarrafi@smu.edu), PhD candidate, and R. KOVACEVIC (kovacevi@lyle.smu.edu), professor, are with the Research Center for Advanced Manufacturing, Southern Methodist University, Dallas, Tex.

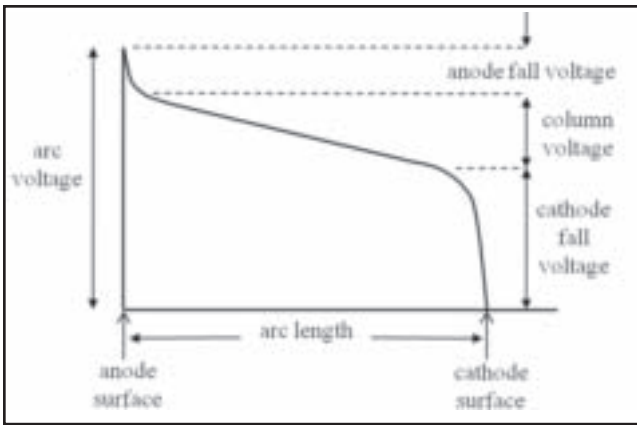


Fig. 1 — Typical distribution of arc voltage (modified from Ref. 13).

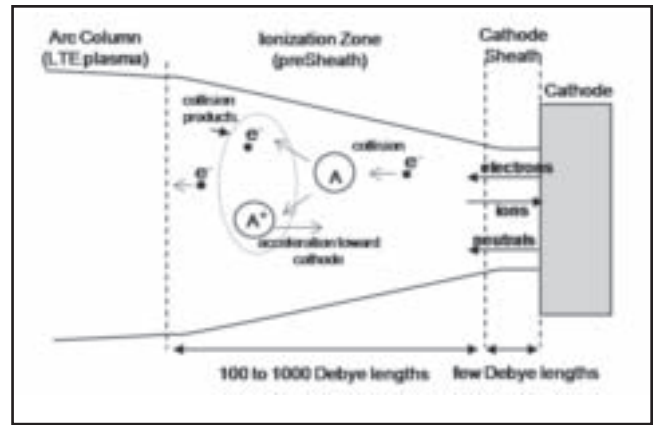


Fig. 2 — General configuration of cathode region of an arc, not true to scale (adapted from Ref. 11).

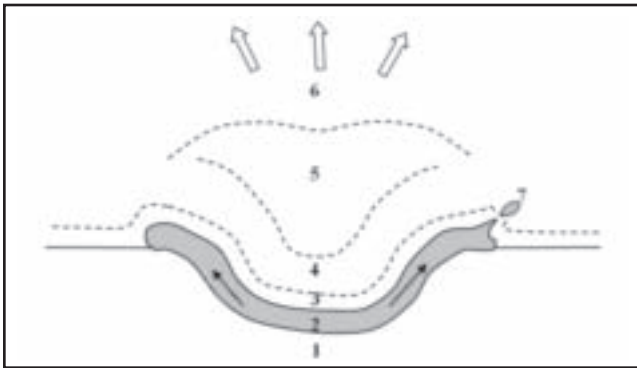


Fig. 3 — Schematic drawing of the cross section of a cathode spot (not true to scale, redrawn from Ref. 16). 1 — Metal cathode under spot (solid), 2 — molten metal layer (0.2–0.5 μm), 3 — cathode sheath (less than 0.01 μm), 4 — presheath (0.1–0.5 μm), 5 — dense plasma over cathode spot, 6 — plasma expansion region, 7 — ejection of molten droplets.

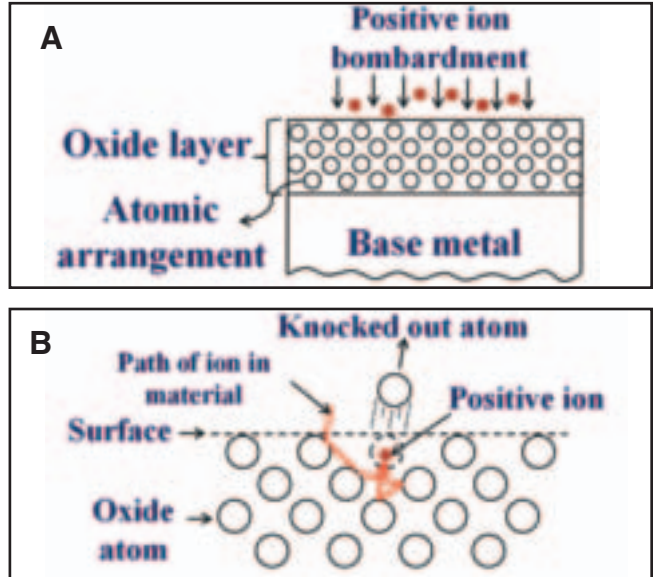


Fig. 4 — Schematic drawing of sputtering mechanism performed by incident ions from plasma. A — The schematic drawing of bombarding ions and material lattice; B — possible ejection of a surface atom by a reflected ion.

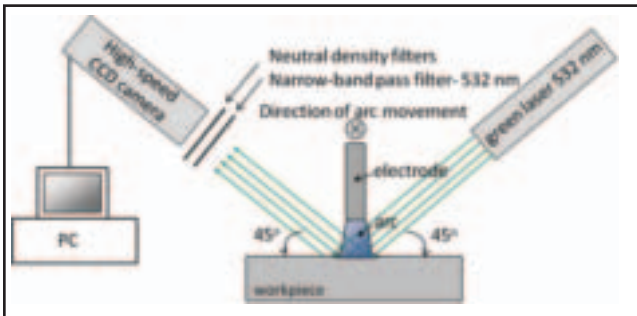


Fig. 5 — Schematic drawing of the machine-vision system.

zone). The presheath is responsible for the generation of charged particles while the cathode sheath is responsible for some important electric processes of the cathode region (Ref. 11). The overall thickness of the cathode region is about 100 to 1000 Debye lengths. “The Debye length is the characteristic distance in a plasma beyond which the electric field of a charged particle is shielded by particles having charges of the opposite sign” (Ref. 12). The Debye length is about 10^{-8} m in the argon atmospheric arc (Ref. 11).

ode fall voltage, 2) the ions formed in the presheath and accelerated toward the negative cathode, and 3) some plasma electrons that reach the cathode surface by diffusion in the reverse direction of the potential gradient. Generally, the attraction of ions by the negative cathode and repulsion of electrons from it cause the formation of a net positive charge in the cathode sheath (so-called space charge). The presence of a positive space charge establishes high electric fields in the vicinity of cathode surface, which in turn helps sustain

the electron emission from the cathode, and therefore assists continuation of the arc.

Arc cathodes can be categorized into two types based on their electron emission mechanism: thermionic and nonthermionic. The thermionic emission mechanism refers to the emission of surface electrons when they overcome the bonding energies in high temperatures and detach from the material as a consequence. Only specific types of refractory materials such as tungsten and molybdenum (thermionic cathodes) can withstand the high temperatures necessary for thermionic emission. The lower boiling-point materials (nonthermionic cathodes) such as aluminum, iron, and copper undergo a phase transformation and evaporate before very high temperatures can be generated on their surface. Although nonthermionic cathodes cannot withstand very high temperatures, it is reported that these

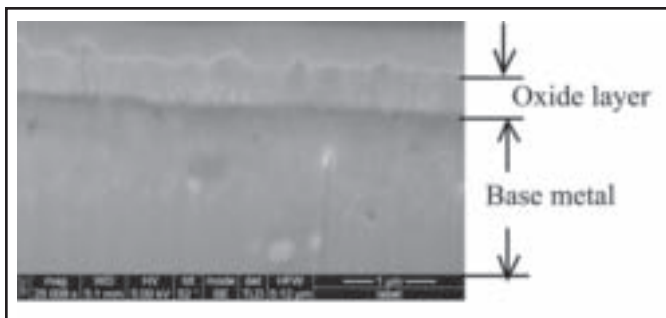


Fig. 6 — FIB-cut cross section of the sample surface showing the initial condition of surface oxide.

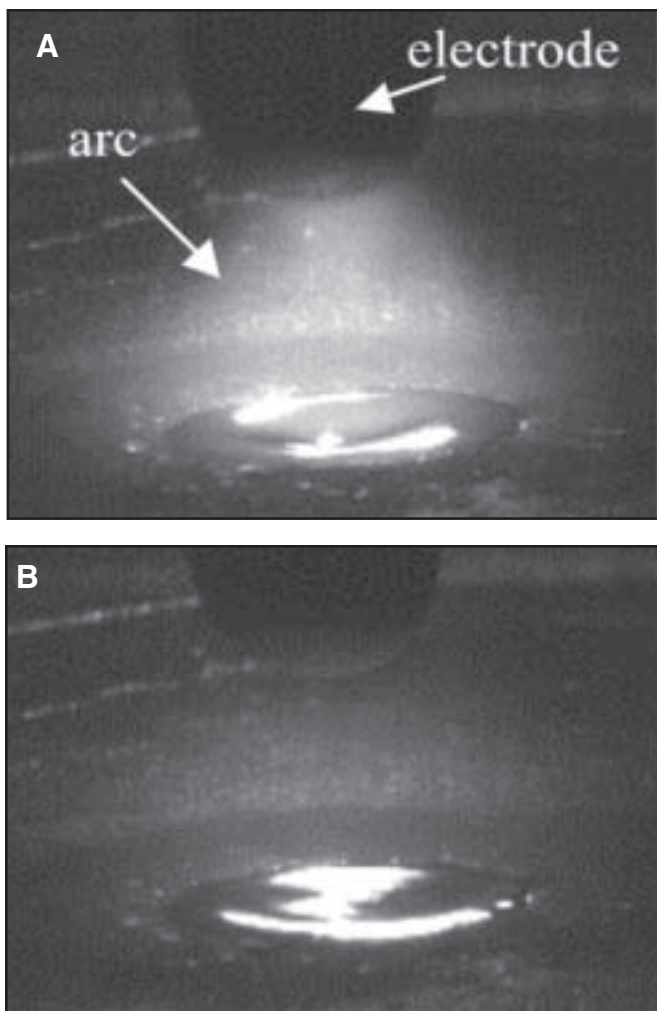


Fig. 7 — Variable-polarity arc in DCEN and DCEP polarities. A — DCEN polarity; B — DCEP polarity.

cathodes can provide very high electron emission rates (high currents) by the thermo-field emission mechanism (Ref. 11). In the thermofield emission mechanism, the synergic effect of high temperatures and a strong electric field creates a high electron current. The thermofield emission is basically a temperature-assisted field emission mechanism. In this mechanism, the electrons escape the surface under the influence of a strong electric field through the quantum mechanical effect of tunneling (field

emission) and overcome the energy barrier that is significantly reduced under the effect of a high temperature. The strong electric field (e-field) and high thermal energy concentration needed for the thermofield emission can only be met locally in cathode spots on the nonthermionic cathodes. In fact, the current is localized at a number of tiny spots (a few μm) in order to provide the high temperature and e-field necessary for a sustainable production of arc current by a relatively cold surface of a nonthermionic cathode. Therefore, the generation of cathode spots is necessary for supplying the arc current from a nonthermionic cathode.

Very high rates of material evaporation have been reported at the cathode spots (Refs. 11, 14) because of the high energy density (10^{10} to 10^{11} $\text{A}\cdot\text{m}^{-2}$ current density (Refs. 11, 15)). The intensive evaporation accompanying the formation of cathode spots is shown to be necessary for the electron generation by cold cathodes (Ref. 14). The high evaporation rate and the high level of energy available for

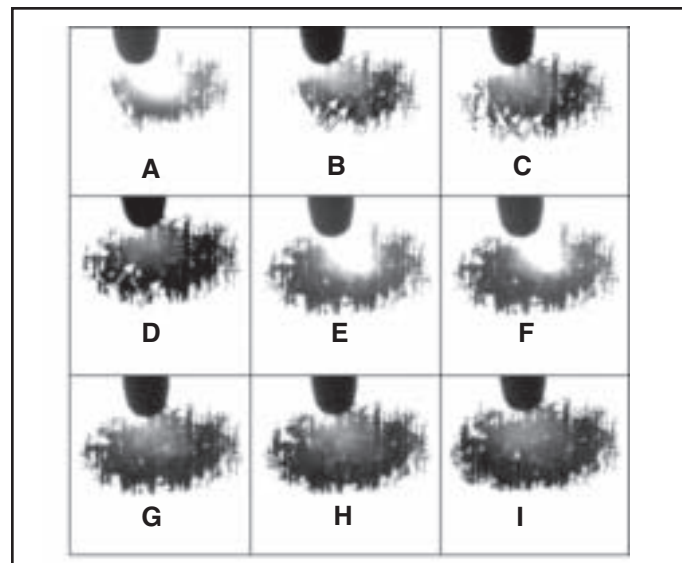


Fig. 8 — The arc and the affected zone during a few subsequent DCEN and DCEP pulses at the initial current cycles after the arc ignition. A, E, and F — DCEN polarity; B–D and G–I — consecutive images during two DCEP pulses. The interval between images is 3.3 ms, except the interval between E and F, which is 20 ms.

ionizing the evaporated atoms together provide a high density of positive ions on the surface of the cathode spot, which in turn generates the high e-field required for thermofield emission (Refs. 11, 14). A schematic cross section of a cathode spot is shown in Fig. 3 (Ref. 16). The extensive evaporation can push the liquid material out of the cathode spot, and a crater may be left as a result — Fig. 3. The ejection of droplets out of the cathode spots may also occur — Fig. 3, item 7.

The region of arc attachments to the nonthermionic cathode can consist of a number of spots. For example, Coulombe (Ref. 11) shows that the arc is attached to the copper cathode through a number of mobile macroscale spots (much bigger than a single cathode spot); each of which consists of several microspots. The lifetime of a macroscale spot is much higher than that of small cathode spots (ms compared to μs) (Ref. 11).

The cathode spots, which are the attachment points of arc to nonthermionic cathodes, are highly mobile unlike the attachment point of the arc to the thermionic cathode. The attachment point of the arc to the thermionic cathode is a relatively large, fixed area (Refs. 11, 15). The cathode spots usually do not stay in their place more than a few microseconds. They repeatedly extinguish and reignite on the neighboring surface of nonthermionic cathodes. In contrast, in thermionic cathodes, the arc attachment covers a large area and is fixed. The reason for the mobility of the cathode spots is not well understood. However, studies of the cathode spots in vacuum arcs show that a certain degree of randomness exists in the motion

ionizing the evaporated atoms together provide a high density of positive ions on the surface of the cathode spot, which in turn generates the high e-field required for thermofield emission (Refs. 11, 14). A schematic cross section of a cathode spot is shown in Fig. 3 (Ref. 16). The extensive evaporation can push the liquid material out of the cathode spot, and a crater may be left as a result — Fig. 3. The ejection of droplets out of the cathode spots may also occur — Fig. 3, item 7.

The region of arc attachments to the nonthermionic cathode can consist of a number of spots. For example, Coulombe (Ref. 11) shows that the arc is attached to the copper cathode through a number of mobile macroscale spots (much bigger than a single cathode spot); each of which consists of several microspots. The lifetime of a macroscale spot is much higher than that of small cathode spots (ms compared to μs) (Ref. 11).

The cathode spots, which are the attachment points of arc to nonthermionic cathodes, are highly mobile unlike the attachment point of the arc to the thermionic cathode. The attachment point of the arc to the thermionic cathode is a relatively large, fixed area (Refs. 11, 15). The cathode spots usually do not stay in their place more than a few microseconds. They repeatedly extinguish and reignite on the neighboring surface of nonthermionic cathodes. In contrast, in thermionic cathodes, the arc attachment covers a large area and is fixed. The reason for the mobility of the cathode spots is not well understood. However, studies of the cathode spots in vacuum arcs show that a certain degree of randomness exists in the motion

The cathode spots, which are the attachment points of arc to nonthermionic cathodes, are highly mobile unlike the attachment point of the arc to the thermionic cathode. The attachment point of the arc to the thermionic cathode is a relatively large, fixed area (Refs. 11, 15). The cathode spots usually do not stay in their place more than a few microseconds. They repeatedly extinguish and reignite on the neighboring surface of nonthermionic cathodes. In contrast, in thermionic cathodes, the arc attachment covers a large area and is fixed. The reason for the mobility of the cathode spots is not well understood. However, studies of the cathode spots in vacuum arcs show that a certain degree of randomness exists in the motion

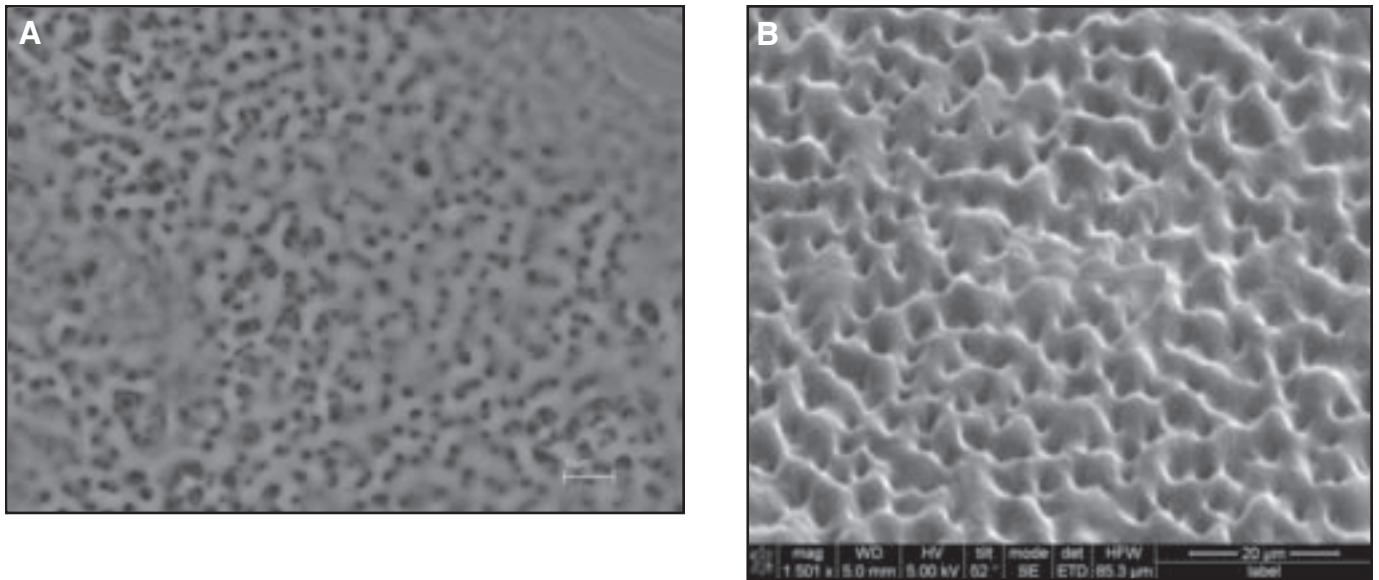


Fig. 9 — A — SEM image of a surface that is cathodically cleaned by variable-polarity arc, top view; B — SEM image of a surface that is cathodically cleaned by variable-polarity arc, tilted view.

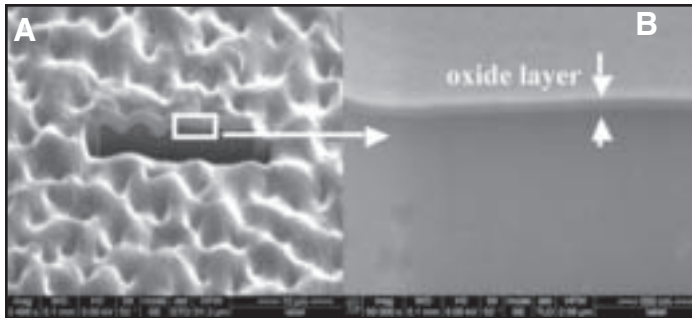


Fig. 10 — FIB-cut section of the arc-treated surface. A — FIB section of the cleaned surface (white layer covering the surface is the protective layer); B — high-magnification image of the section.

of the cathode spots on the cathode surface (Ref. 17). The intensive evaporation at the cathode spots and their high mobility lead to the erosion of nonthermionic cathodes. The erosion of nonthermionic cathodes is currently an active field of plasma physics research. The cathode spots can also be formed on the nonthermionic cathodes covered with dielectric films such as oxides (Ref. 11).

Mechanism of Cathodic Cleaning during Aluminum Welding

Three main mechanisms are suggested in the literature of aluminum welding to describe the cathodic cleaning of oxides during the electrode positive polarity. According to the first suggested mechanism (Refs. 3, 10, 18), the positive ions that are accelerated toward the aluminum cathode are assumed to “sputter” the surface oxide layer. Sputtering is the ejection of substrate atoms by the effect of the high-energy bom-

arding particles. In the second hypothesis (Ref. 19), the surface oxides are assumed to be destroyed because of the dielectric breakdown phenomenon, which is often destructive to the dielectric medium, is called dielectric breakdown. In the third hypothesis, which can be found in more recent literature (Ref. 20), the evaporation of the oxide layers at the cathode spots of nonthermionic cathodes is considered to be a possible mechanism for cathodic cleaning. However, there is no paper in literature dedicated to the experimental investigation using the direct observation method of the physical processes underlying the cathodic cleaning of oxides by a welding arc.

Sputtering is the ejection of substrate atoms from their lattice under the effect of high-energy bombarding particles. In the case of the sputtering of cathode material in the plasma of arcs and glow discharges, the energetic positive ions striking the surface are responsible for the removal of atoms from the substrate — Fig. 4. Some of the energetic incident ions can penetrate into the interatomic space of the substrate material lattice, experi-

ence a number of collisions (Fig. 4B), and even start a cascade of collisions inside the material. They can also accelerate the surface atoms of substrate into the material, and these atoms can ignite multiple collisions themselves. A portion of these atoms and ions can bounce upward and knock out the surface atoms — Fig. 4B.

Sputtering is an atomistic process in nature. The Monte Carlo modeling approach is used in literature to predict the sputtering phenomenon (Refs. 21, 22). The software *TRIM* (transport of ions in matter) (Ref. 21) was developed based on the Monte Carlo binary collision approach. The incident ions and all atoms they collide with are tracked within a finite volume of material by this program. Atoms and ions are followed until their energy is damped below a certain level needed to escape the lattice (Ref. 23). When either the reflected ion or atom reaches the surface and hits a surface atom, the energy of the hitting particle is compared with the surface binding energy of the material by the program. If the particle energy in the perpendicular direction exceeds the surface binding energy, the struck atom escapes the material and is sputtered. If the energy of the striking particle is less than the surface binding energy, it is reflected back into the bulk of material and the process continues (Ref. 23). This program has shown a high degree of accuracy for incident particles of less than 1000 eV energy (Ref. 23). The sputtering method is used as an etching process (e.g., in the semiconductor industry), and as a thin film deposition process, where the sputtered atoms are transferred to be deposited on the desired location. Usually, ions within the energy range of

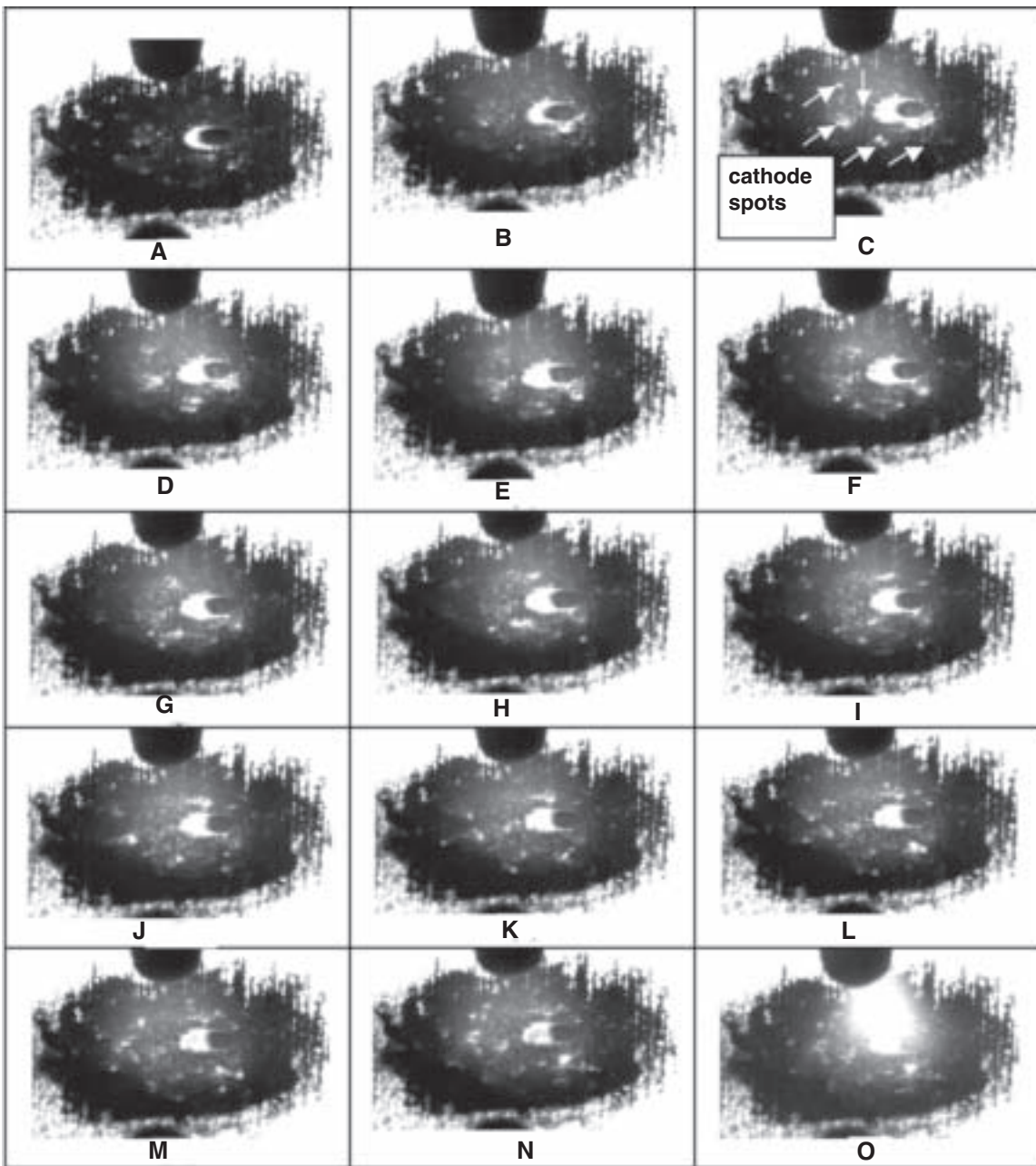


Fig. 11 — The evolution and mobility of cathode spots during a single DCEP polarity of the arc after 1 s from arc ignition; current = 180 A, DCEP duty cycle = 0.4, frequency = 30 Hz.

300–800 eV are used for sputtering (Ref. 23).

The sputtering of the aluminum oxide

Table 1 — Process Parameters Tested in the Experiments

Test Parameter	Level 1	Level 2	Level 3
Current level (A)	90	120	180
DCEP duty cycle	0.1	0.2	0.3
Frequency (Hz)	30	60	90

layer by positive ions was the first mechanism hypothesized for the cathodic cleaning (Refs. 3, 18). Herbst (Ref. 18) qualitatively describes the cathodic cleaning as a miniature sandblast. The most important evidence to form this hypothesis is the observation of the higher rate of cleaning when argon shielding gas is used compared to the case of helium gas. Later, Pattee et al. (Ref. 3) performed a statistical and thermal analysis of the arc and suggested that sputtering can qualitatively be responsible for cathodic cleaning.

After the advancement of sputtering

models and development of accurate simulation programs that could predict the sputtering yields accurately, Pang et al. (Refs. 19, 24) calculated the sputtering yield of aluminum oxide by the welding arc plasma using *TRIM* software. The sputtering yield obtained by bombarding ions of the welding arc was too low to be responsible for the cathodic cleaning of oxides. According to the computations of Pang (Ref. 19, 24), ions with at least 45 eV of kinetic energy are needed to obtain a considerable rate of oxide removal. For the welding arc, they assumed a maximum of 2 eV from

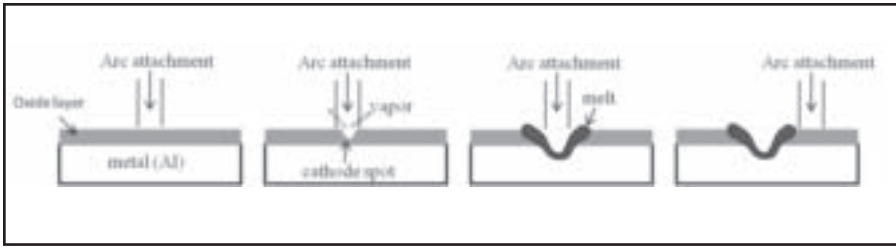


Fig. 12 — Schematic presentation of the mechanism of cathodic cleaning of oxides by mobile cathode spots, not true to scale (inspired from the work of Arai et al. Ref. 31).

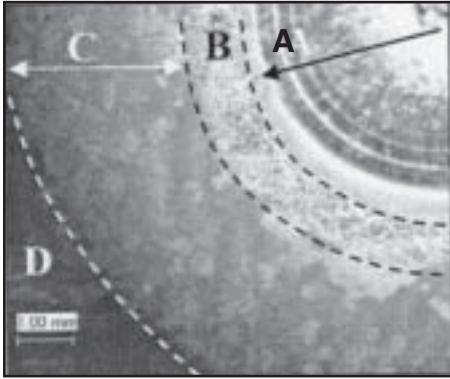


Fig. 13 — Different areas formed on the surface after its melting by variable-polarity arc. A — Molten pool; B — shiny, cleaned, smooth surface adjacent to the molten pool; C — rough, cleaned surface; D — not affected.

thermalization, and a maximum of 8 eV for the cathode fall voltage, which accounts for a maximum total energy of 10 eV for incident ions. The assumption of 2 eV of thermalization energy for positive ions is based on the spectroscopic measurement of arc temperature by Pang et al. (Ref. 24). The computational work of Pang et al. (Refs. 19, 24) suggests that sputtering is improbable to be the mechanism of cathodic cleaning. Some information on the measurement of the thermal energy of ions is presented in the next paragraph.

The average energy of the bombarding ions is often considered to be the superposition of the thermal energy (gained in the presheath and arc column) and the kinetic energy (gained in the cathode fall zone) (Ref. 11). The measurement of arc temperature can provide the average thermal energy of ions. Because the condition in the column of the atmospheric arc is close to the local thermodynamic equilibrium state (Ref. 25), the electron temperature in the arc column is almost equal to the ion temperature, and the measurement of the electron temperature can provide a good estimate of the ion temperature in this zone. The electron temperature of the arc plasma can be approximated using an emission spectroscopy technique.

After rejecting the sputtering mecha-

nism through a TRIM simulation, Pang et al. (Ref. 19) proposed the dielectric breakdown as the possible mechanism of cathodic cleaning. However, no evidence for the dielectric breakdown process being responsible for oxide removal is shown in the paper.

The cathode spots of a vacuum arc can remove surface contaminations and dielectric layers from the surface of a nonthermionic cathode (Refs. 26–28). Coulombe (Ref. 11) reports that the cathode spots can play the same role in an atmospheric arc with a nonthermionic cathode. However, the applicability of this mechanism is not well investigated in the welding context. Scotti et al. (Ref. 20) discussed the possibility of the cathode spots being the mechanism of cathodic cleaning. However, the focus of their report is the effect of cathodic cleaning on the arc stability and bead formation, and the basic mechanism of cathodic cleaning is not addressed in their work.

In the papers and books related to welding, an uncertainty about the mechanism of cathodic cleaning is still observed. Several papers (Refs. 3, 18–20) discuss the possibility of some mechanisms being responsible for cathodic cleaning, but these mechanisms are not evaluated in a single report. Because there is no direct observation of the mechanism of cathodic cleaning, it has been difficult to determine which mechanism is responsible for the cathodic cleaning. Direct real-time observation of cathodic cleaning can provide a better understanding of this process compared to the investigations performed after extinguishing the arc. The purpose of this paper is to study the mechanisms of cathodic cleaning by directly observing the cleaning process using a high-speed machine-vision system, and examining the surface cleaned by the arc.

Experiments

Al 6061 plates with the dimension of 50 × 30 × 6 mm were used as test coupons. A stationary variable-polarity arc was established between a pure tungsten electrode and the test coupon's surface using a Miller Dynasty DX® square-wave AC power source. A tungsten electrode of 3.2

mm in diameter with a semispherical tip was used. Argon gas with 99.8% purity (industrial grade) and the flow rate of 12 L/min was used as the shielding gas. The arc length was about 3 mm. The variable-polarity arc was ignited for 5 s in each experiment, and its interaction with the surface was recorded with a high-speed CCD camera assisted by a green laser as an illumination source in order to visualize the cathodic cleaning process. Three levels of current, DCEP duty cycles, and frequencies were tested as shown in Table 1. The current levels in DCEP and DCEN polarities were equal. The DCEP duty cycle quantifies the contribution of DCEP polarity duration in one cycle of current.

The main challenge in visualizing the interaction of the arc with the surface is the strong light emission from the arc plasma in a broad range of wavelengths. A combined illumination and filtration approach based on specular reflection was used to overcome this problem. The schematic of the integrated machine-vision system used in this study is shown in Fig. 5. The machine-vision system consists of four main components: 1) a 5-W continuous-mode Coherent Tracer Compact® green laser source (532-nm wavelength) with a collimated light output, which was used to illuminate the surface exposed to the arc; 2) the appropriate neutral-density filters; 3) a narrow-band-pass filter to bypass only the green laser light; and 4) a high-speed CCD camera, which is described in more detail in the next paragraph. Most of the light emitted by the plasma is filtered out by the narrow-band-pass filter, while the green light reflected from the area of interest, which carries the visual data of the processing area, passes through the filter and is captured by the camera.

Because the cathodic cleaning occurs during a very short period of time while the specimen is the cathode of arc, the use of a high-speed camera is needed to capture the events during this process. In this research, a high-speed CCD camera was used with a frame rate of 2074 frames per second (fps) and a frame size of 240 × 240 pixels with a density of 72 pixels per inch. This frame rate allows for taking six consecutive pictures during the DCEP polarity of the arc when the current frequency is 60 Hz and 20% of the current cycle is devoted to the DCEP polarity. The pictures were stored in a PC for studying the interaction of the arc with the specimen's surface.

The machine-vision system used in this research is similar to that used in the work of Sarrafi et al. (Ref. 29) except they used a regular camera (60 fps). They showed that the presence of oxides on the molten pool can be monitored using a machine-

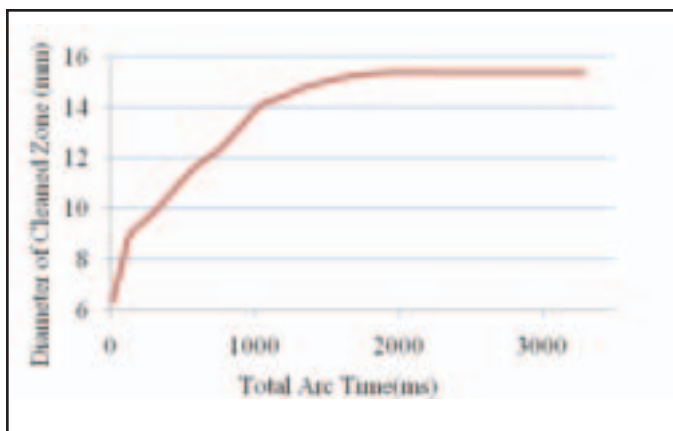
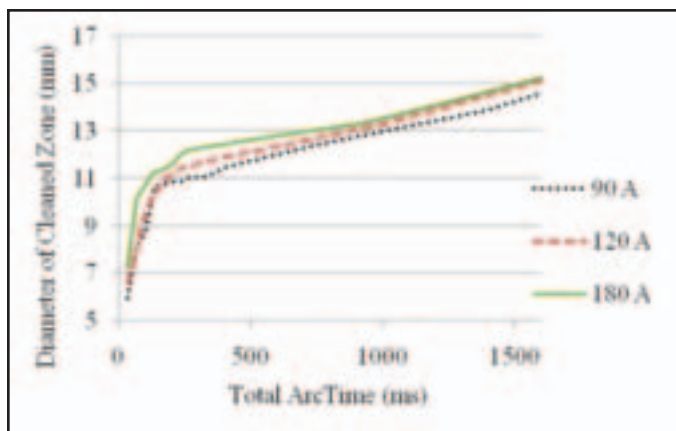


Fig. 14 — The effect of current on the growth of the cleaned zone. Constant parameters: frequency = 30 Hz, DCEP duty cycle = 0.4.

Fig. 15 — The trend of growth of the cleaned zone vs. time in a 3-s time frame. Parameters: current = 180 A, DCEP duty cycle = 0.4, frequency = 60 Hz.

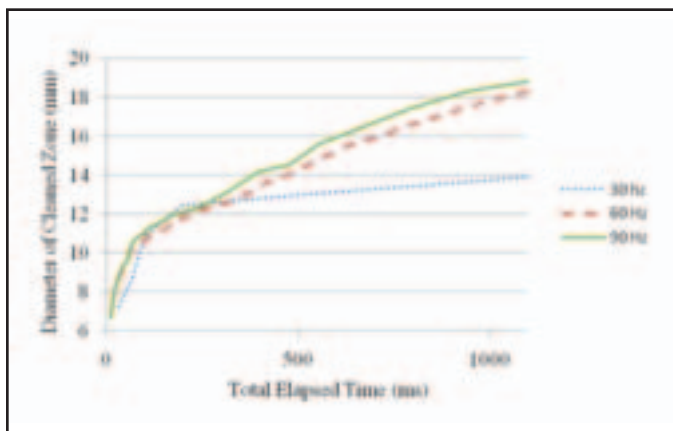
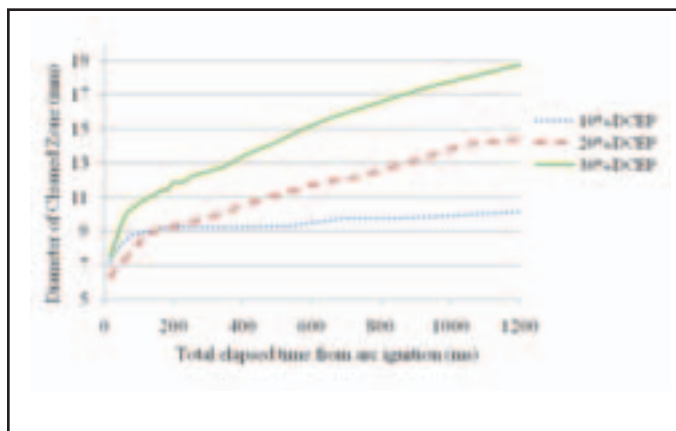


Fig. 16 — The effect of DCEP duty cycle on the diameter of the cleaned zone and its rate of growth. Parameters: current = 180 A, frequency = 60 Hz.

Fig. 17 — The effect of frequency on the diameter of the cleaned zone and its rate of growth. Parameters: current = 180 A, DCEP duty cycle = 0.4.

vision system. The integrated machine-vision system was capable of recognizing the oxide fragments on the top of the molten pool. They also showed that in order to have an oxide-free molten pool during welding, the oxides should be cleaned from the solid surface in front of the molten pool by the cathodic cleaning action of the arc. The selection of process parameters to meet this requirement was also discussed in their research without a detailed explanation of the physical mechanism of cathodic cleaning.

Cathodically cleaned surfaces were examined by optical and scanning electron microscopy. Optical microscopy was used to give an overview of the area affected by the arc. Scanning electron microscopy, which can provide a larger depth of focus, was used to observe the surface topography of the area affected by the arc. A focused ion beam was used to locally cut through different locations of the affected surface in order to measure the average thickness of the surface oxide. An optical profiler based on the chromatic aberration

principle was used to measure surface roughness as needed.

Results and Discussion

Original Condition of Surface Oxide

Figure 6 shows a cross section of the base metal surface cut by a focused ion beam to measure the thickness of the oxide layer existing on the base metal surface. As shown in the picture, the surface of Al 6061 samples was covered by a fairly uniform oxide layer with the thickness between 450 and 500 nm before any treatment by the arc.

Appearance of Arc in DCEN and DCEP Polarities

Figure 7A and B shows the arc during DCEN and DCEP polarities. The arc in DCEN polarity is much brighter than the arc in DCEP polarity as shown in Fig. 7A and B. The low intensity of arc emission during DCEP polarity makes the viewing

through the DCEP arc easier than through the DCEN arc. The observed difference in arc brightness agrees with the conclusion of Pang et al. (Ref. 24) and Qingdong et al. (Ref. 30) that the temperature of the arc column is lower in the DCEP polarity than in the DCEN polarity.

General Observations during Cathodic Cleaning

Figure 8 shows the arc and condition of the affected surface during the initial current cycles after the arc is ignited. Figure 8A was taken during the DCEN polarity. Figure 8B–D are consecutive images of the arc and the affected area on the surface. These images were taken during one DCEP polarity pulse, which was subsequent to the DCEN pulse of Fig. 8A. Figure 8E and F shows the status of the arc and affected area on the surface during the next DCEN pulse, where Fig. 8E shows the beginning of the DCEN period and 8F shows the end of it. Figure 8G–I shows the arc and its effect on the surface

during the DCEP period subsequent to image 8F. The time interval between the images is equal (3.3 ms) except for the interval between the images shown in Fig. 8E and F, which is 20 ms. A darker appearance distinguishes the area affected by the arc from the surface not affected by the arc as seen in Fig. 8. The size and surface conditions of the affected area do not change during DCEN polarity (Fig. 8E, F), but expands during the DCEP polarity (Fig. 8B–D, G–I).

Subsequent surface studies showed the area appearing dark in the real-time images is cleaned from oxides. Figure 9A and B shows the typical SEM images of the surface appearing dark in the real-time images. The porous structure of the surface is probably the cause for the dark appearance of this area. Figure 10A shows a typical focused ion beam (FIB) section of the surface of Fig. 9B. The white layer covering the surface in Fig. 10A is the platinum layer that protects the surface during FIB milling. Figure 10B shows a higher magnification of the section shown in Fig. 10A. Base aluminum, a thin oxide layer, and the protective layer are seen in this figure. As shown in Fig. 10B, the surface oxide layer on the arc-treated area is very thin (40–50 nm) on the arc-treated area. This thin oxide layer cannot be the original oxide layer remaining on the surface but was probably formed after the surface cleaning action of the arc (secondary oxide). Therefore, the dark area in the real-time images is considered cathodically cleaned from oxides.

The images taken during DCEP polarity show the evolution of some bright spots on the oxidized aluminum surface and their movement across the surface (Fig. 8B–D and G–I). The surface images during DCEP polarity also suggest the role of observed mobile bright spots on the removal of surface oxide. The cleaned area grows in synchronization with the movement of bright spots across the surface. What we see as bright spots in these images are the major clusters of cathode spots whose local plasma have intense enough emission. We also see the shiny trace they leave after scanning the surface. The movement of cathode spots is linked to their decay at one surface spot and the re-ignition at the neighboring surface (Refs. 11, 14).

It is worth noting that many cathode spots of different sizes and lengths of duration evolve on the surface of a non-thermionic cathode. What we see in these images are the most energetic clusters of cathode spots that produce bright local plasmas as well as the traces they leave after scanning the surface. Not all of the cathode spots can be seen in the pictures because their visibility can be limited by their short lifetime as well as their very

small size when they cannot gather in big clusters and produce significantly bright local plasma and cannot leave a wide enough trace. The behavior of the visible cathode spots is the basis for discussing the real-time images in this research.

The visibility of cathode spots increases with time. During the initial pulses of DCEP, the cathode spot clusters are small and weak. However, as more pulses of DCEP hit the surface, the spots become larger and cause more surface melting. Figure 11A–N shows the consecutive real-time images of the affected area during DCEP polarity after one second of arc ignition. The spots seen in Fig. 11 are more intense than those seen in Fig. 8. They leave wider traces while scanning the surface and causing more melting. When the cathode spots cause too much surface melting, they can make the surface smoother, as discussed in the following sections.

Based on the real-time observations and surface topography of the cleaned area, it can be concluded that the cathode spots are responsible for the cathodic cleaning of oxides. Real-time high-speed movies clearly show that the cleaned area forms and expands by mobile cathode spots. In fact, the cathode spots sweep the surface and consume the oxides by vaporizing a thin layer of the surface. The topography of the cathodically cleaned surfaces (surfaces of Fig. 9A, B) agree well with the typical surfaces affected by cathode spots as reported in literature (Ref. 31). The cleaned surface consists of an array of micrometer-sized depressions embraced with thin ridges. The depressions seem to be the sites of cathode spots, and the ridges are formed because the pressure of evaporation pushes the liquid out of the cathodes spot (as shown schematically in Fig. 3). Based on the observations, it is hypothesized that the mechanism of cathodic cleaning is similar to the schematic drawing shown in Fig. 12. It is worth noting that this hypothesized mechanism is very general in nature, and the details of the mechanism should evidently be studied in the future. This schematic presentation is similar to the mechanism shown in the work of Arai et al. (Ref. 31) on the cleaning of a metal surface by vacuum arcs.

Surface Condition after Cathodic Cleaning

Different areas are formed on the surface of the aluminum specimen after exposing it to a variable-polarity arc as shown in Fig. 13. A quarter of a weld crater (marked as area A in Fig. 13) is seen at the right upper-corner of the picture. The cathodically cleaned area on the solid surface contains two different zones marked as B and C in Fig. 13. Most of the

cleaned area has a matte appearance (area C in Fig. 13) and is roughened by cathode spots similar to the surface of Fig. 9B. This area appears dark in the real-time images. The arithmetic mean deviation of the roughness profile, R_a , is about 1.8 μm in this area. The cleaned area adjacent to the molten pool (marked as B in Fig. 13) is, however, shiny and smooth. This area appears shinier than area C in real-time images. The arithmetic mean deviation of the roughness profile, R_a , is about 0.7 μm in area B. Scanning electron microscopy showed the sign of extensive surface melting, such as hot cracks, on this area. The real-time images suggest that the smoothness of this area is related to the frequent scanning of this area by the cathode spots, which leads to extensive surface melting. The real-time images suggest that the density of the cathode spots is lower at areas located farther from the arc axis compared to areas located closer to it. Therefore, in areas located farther from the arc center, such as area C, the cathode spot marks are usually individual. Whereas, on areas closer to the arc center, such as area B, the frequent scanning of the surface by cathode spots and a higher heat input during DCEN polarity cause a uniform surface melting that makes the surface smooth. The area marked as D in Fig. 13 is not affected by the arc.

The Behavior of Cathode Spots during Cathodic Cleaning of Oxides

As already stated in the literature of plasma physics, the behavior of cathode spots of nonthermionic cathodes is highly sensitive to local surface conditions (surface layers, surface dirt and oil, oxide condition, roughness, and surface defects), electrode material, shielding gas composition, and its impurity (Refs. 11, 15). The absolute numerical values related to the cathode spots behavior, therefore, may easily vary by a small change in the experimental conditions. Thus, in this paper, the focus is not on the absolute values in describing the cathode spots behavior, but the trends in their behavior.

Based on the pictures taken by high-speed camera, the cathode spots occur everywhere on the surface covered by the atmospheric arc of welding; they can form on the surface with the original oxide, as well as on the surface already scanned by cathode spots. Literature (Refs. 26, 28, 31, 32) reports an opposite behavior of cathode spots in the case of a vacuum arc. It is reported that when an area is scanned by cathode spots of a vacuum arc and cleaned from the surface impurities, the cathode spots seldom come back to that area (Refs. 26, 28, 31, 32). Therefore, the cathode spots of the vacuum arc preferentially attack the surfaces that are not yet scanned

by cathode spots, which is referred to as the “intelligent” behavior of the vacuum arc during cleaning (Ref. 31). The surface oxide layers are supposed to facilitate the thermo-field emission because of the generation of a high electric field (Ref. 11) as well as their lower work function compared to metals (Refs. 10, 32). The vacuum arc needs a voltage increase at the completion of oxide cleaning in order to be sustained (Ref. 33), or it may be extinguished at this stage (Ref. 10). The surface oxide layers feed the cathode spots of the arc during DCEP polarity and help sustain the DCEP arc. In the welding arc, the re-formation of cathode spots on the surface already scanned by cathode spots could be related to the re-oxidation of previously-treated areas (the quick formation of very thin layers of oxide on the surface already scanned by cathode spots). Further experimental confirmation is needed to verify this hypothesis. Based on the frequent occurrence of the welding arc cathode spots on the surfaces that are already scanned, it can be said that the vacuum arc acts “more intelligently” and more efficiently in cleaning oxides compared to the atmospheric arc of welding. However, the cleaning efficiency of a variable-polarity atmospheric arc is practically sufficient for welding purposes.

Real-time pictures show two distinct phases in the behavior of cathode spots during each single pulse of DCEP. At the beginning of the DCEP pulse (the first 0.5 ms of each DCEP polarity period), cathode spots are formed randomly on the surface. We may call the first phase as the random hit of cathode spots. Then, an outward movement of cathode spots from the center to the edge of the cleaned area is observed until the end of the DCEP polarity pulse. In the second phase, the cathode spots are more visible (have a brighter plasma) and leave shinier traces. The expansion of the cleaned zone occurs during both phases of a DCEP pulse.

As already stated, the high-speed camera images show that the surface affected by the arc expands during the DCEP period of the arc. The area cleaned by the VP arc nonlinearly varies with time when the surface is treated by many pulses of DCEP. The growth of the cleaned zone is very fast at the first few pulses of DCEP current but slows down later, as shown in Fig. 14. In the experiments, when the diameter of the cleaned zone reaches some value between 9 and 12 mm, the cleaned zone continues to grow linearly at a lower rate, as shown in Fig. 14. Tracking the variation of the diameter of the cleaned zone in a longer timeframe showed that the growth of the cleaned zone stops after a certain diameter is cleaned. For a typical case ($I = 180$ A, DCEP duty cycle = 0.2, and frequency = 60 Hz), the growth of the

cleaned zone over time nearly stopped when the size of the cleaned zone reached about 15.5 mm, as shown in Fig. 15.

Increasing the current level enlarges the cleaned zone, but the difference is not significant, as shown in Fig. 14. Images show that when the current level increases, the cathode spots become stronger with a higher level of energy, especially during the second phase of the cathode spots behavior (the phase during which the outward movement of spots occurs).

Figure 16 shows the significant effect of the DCEP duty cycle on the size of the cleaned zone and its rate of growth. Increasing the DCEP duty cycle enlarges the cleaned zone and quickens its rate of growth. Images show that increasing the DCEP duty cycle provides more time for the cathode spots to move around on the surface and expand the cleaned zone.

As typically shown in Fig. 17, varying the frequency does not cause a significant change in the diameter of the cleaned zone at the beginning of arc ignition, but causes significant variation in the growth rate of the cleaned zone in the longer run. The change in the rate of growth is especially significant when the frequency increases from 30 to 60 Hz. A higher frequency provides a higher number of DCEP pulses with a shorter length compared to a lower frequency. Images suggest that increasing the frequency causes a faster growth of the cleaned area by providing a higher number of random hits of the cathode spots (phase 1 of the DCEP polarity period).

Conclusions

The mechanism of the cathodic cleaning of oxides from aluminum surface variable-polarity arc was investigated in real-time using a machine-vision system and a high-speed camera (about 2000 fps). Surface studies were also performed after the cathodic cleaning process. The following conclusions can be drawn based on the experiments:

1) The surface oxide layer is removed by the mobile cathode spots during the DCEP polarity.

2) The cathode spots of the welding arc form on the oxides that originally exist on the specimen's surface and the areas already scanned by the cathode spots.

3) The specimen's surface after welding with the variable-polarity arc consists of three distinct regions: 1) molten metal; 2) a cleaned, smooth surface adjacent to the weld pool, where repetitive scanning by cathode spots caused smoothness; and 3) a rough, porous, cleaned surface located farther from the arc center, where craters are related to the locations of the cathode spots.

4) Two phases of cathode spots behav-

ior were observed during each DCEP polarity period. At the very beginning of a DCEP pulse (first 0.5 ms), the cathode spots randomly form on different locations on the surface (the first phase). Then, a number of stronger cathode spots form at the surface close to the arc center and grow outward (the second phase). The expansion of the cleaned zone occurs during both phases.

5) With a stationary arc, the cleaned zone expands nonlinearly with the elapsed arcing time. During the initial pulses of DCEP, the rate of expansion is very fast. Later on, this rate decreases, and subsequently, after reaching a certain diameter, the cleaned zone stops expanding.

6) Increasing the current level, frequency, and DCEP duty cycle in the tested range enlarged the cleaned zone. The DCEP duty cycle has the most significant role on the size of the cleaned zone.

Acknowledgments

This work was financially supported by NSF's Grant EEC-0541952. The work of Andrew Socha, research engineer at the Research Center for Advanced Manufacturing, in the design and integration of the machine-vision system is highly appreciated. The authors would like to thank David N. Ruzic, professor at the University of Illinois at Urbana-Champaign, for his valuable guidance.

References

1. Mathers, G. 2002. *The Welding of Aluminium and Its Alloys*. pp. 22–24, Woodhead Publishing Ltd., Cambridge, UK.
2. Dickerson, P. B. 1993. Welding of aluminium alloys. *ASM Handbook*, vol. 6, pp. 722–739, ASM International, Materials Park, Ohio.
3. Pattee, H., Meister, R., and Monroe, R. 1968. Cathodic cleaning and plasma arc welding of aluminium. *Welding Journal* 47(5): 226-s to 233-s.
4. Sarrafi, R., Lin, D. C., Levert, E., and Kovacevic, R. 2008. Feasibility study of the repair of aluminum components by variable polarity GTAW cladding. *Proceedings of Materials Science and Technology (MS&T 2008) Conference*, Pittsburgh, Pa.
5. Sarrafi, R., Lin, D., Kovacevic, R., and Levert, E. 2008. Significance of reverse polarity in the repair of aluminum components using variable polarity gas tungsten arc welding process. *Proceedings of Conference of Metallurgists COM 2008*, Winnipeg, Canada.
6. Ouyang, J., Wang, H., and Kovacevic, R. 2002. Rapid prototyping of 5356-aluminum alloy based on variable polarity gas tungsten arc welding: Process control and microstructure. *Journal of Materials and Manufacturing Processes* 17(1): 103–124.
7. Wang, H., Jiang, W., Ouyang, J., and Kovacevic, R. 2004. Rapid prototyping of 4043 Al

alloy by VP-GTAW. *Journal of Materials Processing Technology* 148(1): 93–102.

8. Jarvis, B., and Ahmed, N. 1998. The behavior of oxide films during gas tungsten arc welding of aluminum alloys. *Proceedings of International Conference on Trends in Welding Research*, Georgia, pp. 410–414.

9. Ryazantsev, V., Slavin, G., and Ovchinnikov, V. 1992. Formation and failure of oxide films on aluminum alloys. *Welding International* 6(6): 468–470.

10. Lancaster, J. F. 1986. *The Physics of Welding*, second edition, Pergamon Press.

11. Coulombe, S. 1997. A model of the electric arc attachment on non-refractory (cold) cathodes. PhD thesis, Department of Chemical Engineering, McGill University, Montreal, Canada.

12. Parker, S. P. 2003. McGraw-Hill *Dictionary of Scientific and Technical Terms*, 6th ed., McGraw-Hill Companies Inc.

13. Guile, A. E. 1971. Arc-electrode phenomena. *Proceeding of Institute of Electrical Engineers*, 118(9R).

14. Coulombe, S., and Meunier, J. L. 1997. Importance of high local cathode spot pressure on the attachment of thermal arcs on cold cathodes. *IEEE Transactions on Plasma Science* 25(3): 913–918.

15. Fridman, A., and Kennedy, L. A. 2004. *Plasma Physics and Engineering*, chapter 8, arc discharges, Taylor & Francis.

16. Boxman, R. L., Sanders, D. M., Martin, P. J., and Lafferty, J. M. 1995. *Handbook of Vacuum Arc Science and Technology*, Noyes Publications.

17. Anders, A. 2005. The fractal nature of vacuum arc cathode spots. *IEEE Transactions*

on Plasma Science 33(5): 1456–1464.

18. Herbst, H. T. 1948. Electrical characteristics of the arc in Heliarc welding. *Welding Journal* 27(8): 600.

19. Pang, Q., Pang, T., McClure, J. C., and Nunes, A. C. 1994. Workpiece cleaning during variable polarity plasma arc welding of aluminum. *Journal of Engineering for Industry* 116(4): 463–466.

20. Scotti, A., Dutra, J. C., and Ferraresi, V. A. 2000. The influence of parameter settings on cathodic self-etching during aluminum welding. *Journal of Materials Processing Technology* 100(1): 179–187.

21. Biersack, J. P., and Haggmark, L. G. 1980. A Monte Carlo computer program for the transport of energetic ions in amorphous targets. *Nuclear Instruments and Methods* 174: 257.

22. Biersack, J. P., and Eckstein, W. 1984. Sputtering studies with the Monte Carlo program TRIM.SP. *Journal of Applied Physics*, A34, p. 73.

23. Ruzic, D. N. 1990. Fundamentals of sputtering and reflection. *Handbook of Plasma Processing Technology*, edited by S. M. Rossnagel, J. J. Cuomo, and W. D. Westwood, Noyes Publications.

24. Pang, Q. 1991. In situ spectroscopic measurements of variable polarity plasma arc welding on aluminum 2219. MS thesis, Department of Metallurgical and Materials Engineering, University of Texas at El Paso.

25. Pfender, E. 1992. Plasma generation by electric arcs — an overview. *Thermal Plasma Applications in Materials and Metallurgical Processing*, edited by N. El-Kaddah, TMS Publication.

26. Beilis, I. I. 2001. State of the theory of

vacuum arcs. *IEEE Transactions on Plasma Science* 29(5): 657–670.

27. Guile, A. E., and Juttner, B. 1980. Basic erosion processes of oxidized and clean metal cathodes by electric arcs. *IEEE Transactions on Plasma Science* 8(3): 259–269.

28. Shi, Z., Jia, S., Wang, L., Yuan, Q., and Song, X. 2008. Experimental investigation on the motion of cathode spots in removing oxide film on metal surface by vacuum arc. *Journal of Physics D: Applied Physics* 41(17): 175–209.

29. Sarrafi, R., Lin, D. C., and Kovacevic, R. 2009. Real-time observation of cathodic cleaning during variable-polarity gas tungsten arc welding of aluminum alloy. Article in press, *Proceedings of the Institution of Mechanical Engineers, Part B: Journal of Engineering Manufacture*.

30. Qingdong, P., and McClure, J. C. 1991. Emission spectrum and resistivity of low power plasma weld arcs. *Spectroscopy Letters* 24(4): 487–497.

31. Arai, Sugimoto, M., Sugiyama, S., Ishizaka, K., and Takeda, K. 2008. Cathode spot craters in pulse vacuum arc cleaning of a metal surface oxide layer. *Surface and Coatings Technology* 202(22–23): 5293–5297.

32. Takahashi, H., Nakamura, T., Sugimoto, M., and Takeda, K. 2004. Effect of pressure on the behavior of cathodes spots in oxide removal by arc discharge. *Proceedings of International Symposium on Discharges and Electrical Insulation in Vacuum, ISDEIV*, vol. 2, pp. 587–590.

33. Takeda, K., and Takeuchi, S. 1997. Removal of oxide layer on metal surface by vacuum arc. *Materials Transactions – JIM* 38(7): 636–642.

Preparation of Manuscripts for Submission to the *Welding Journal* Research Supplement

All authors should address themselves to the following questions when writing papers for submission to the *Welding Research Supplement*:

- Why was the work done?
- What was done?
- What was found?
- What is the significance of your results?
- What are your most important conclusions?

With those questions in mind, most authors can logically organize their material along the following lines, using suitable headings and subheadings to divide the paper.

1) **Abstract.** A concise summary of the major elements of the presentation, not exceeding 200 words, to help the reader decide if the information is for him or her.

2) **Introduction.** A short statement giving relevant background, purpose, and scope to help orient the reader. Do not duplicate the abstract.

3) **Experimental Procedure, Materials, Equipment.**

4) **Results, Discussion.** The facts or data obtained and their evaluation.

5) **Conclusion.** An evaluation and interpretation of your results. Most often, this is what the readers remember.

6) Acknowledgment, References and Appendix.

Keep in mind that proper use of terms, abbreviations, and symbols are important considerations in processing a manuscript for publication. For welding terminology, the *Welding Journal* adheres to AWS A3.0:2001, *Standard Welding Terms and Definitions*.

Papers submitted for consideration in the *Welding Research Supplement* are required to undergo Peer Review before acceptance for publication. Submit an original and one copy (double-spaced, with 1-in. margins on 8 1/2 x 11-in. or A4 paper) of the manuscript. A manuscript submission form should accompany the manuscript.

Tables and figures should be separate from the manuscript copy and only high-quality figures will be published. Figures should be original line art or glossy photos. Special instructions are required if figures are submitted by electronic means. To receive complete instructions and the manuscript submission form, please contact the Peer Review Coordinator, Erin Adams, at (305) 443-9353, ext. 275; FAX 305-443-7404; or write to the American Welding Society, 550 NW LeJeune Rd., Miami, FL 33126.